

Title	SCALING BEHAVIOR IN EVOLVING CELLULAR STRUCTURES WITH ANISOTROPY(Session IV : Structures & Patterns, The 1st Tohwa University International Meeting on Statistical Physics Theories, Experiments and Computer Simulations)
Author(s)	Nagai, Tatsuzo
Citation	物性研究 (1996), 66(3): 616-617
Issue Date	1996-06-20
URL	http://hdl.handle.net/2433/95751
Right	
Type	Departmental Bulletin Paper
Textversion	publisher

SCALING BEHAVIOR IN EVOLVING CELLULAR STRUCTURES WITH ANISOTROPY

Tatsuzo Nagai

Physics Department, Kyushu Kyoritsu University, Kitakyushu 807, Japan

Many cellular structures in nature can be classified into the isotropic systems, such as soap froths, and the anisotropic systems, such as grain aggregates. The properties of cell boundaries do not depend on the cell states in the former, while those depend on the cell states or the cell orientations in the latter. It has been found so far that we can describe the growth phenomena of the isotropic cellular structures by using the concept of the dynamical scaling from a unified point of view. Few studies exist for the anisotropic systems [1]. Our purpose of this work is to confirm the existence of the dynamical scaling and find its characteristics in the anisotropic systems.

We proposed a deterministic model for cellular structures called the vertex model and studied the growth of the isotropic systems. We will apply this model to the two-dimensional anisotropic system and perform computer simulation [2]. In this model, the system is described as an aggregation of vertices, which are triple points of cell boundaries and are connected with each other by straight boundaries.

The velocity \mathbf{v}_i of the i -th vertex at the position \mathbf{r}_i is given by the equation

$$\sum_j^{(i)} \mathbf{D}_{ij} \cdot (\mathbf{v}_i + \mathbf{v}_j/2) = \sum_j^{(i)} \sigma_{ij} \mathbf{r}_{ji} / |\mathbf{r}_{ji}|, \quad \mathbf{D}_{ij} \equiv \eta_{ij} |\mathbf{r}_{ij}| \mathbf{n}_{ij} \mathbf{n}_{ij}^T / 3, \quad \mathbf{r}_{ij} \equiv \mathbf{r}_i - \mathbf{r}_j,$$

where the sums are over three neighbor vertices of i . The left-hand side of this equation is the friction force where η_{ij} and \mathbf{n}_{ij} are the friction constant and the unit normal vector of the boundary $\langle ij \rangle$, respectively. The right-hand side denotes the driving force, which acts to reduce the total energy of cell boundaries, where σ_{ij} is the energy density of the boundary $\langle ij \rangle$. Furthermore, we describe the topological change of the system by the two elementary processes, the recombination process and the triangle annihilation process, which occur when two vertices collide.

We assume the following orientation dependence: $\sigma_{ij} = 0(0.05 \sigma)$ for $q=q'$; $\sigma_{ij} = \sigma/3$ for $|q-q'| = 2$; $\sigma_{ij} = \sigma$ otherwise, and $\eta_{ij} = \eta$ for all q and q' , ($q=1,2, \dots, 64$). Here q and q' are the orientations of two cells on both sides of the boundary $\langle ij \rangle$ and we introduce a small energy 0.05σ (pseudo boundary) instead of 0 for $q=q'$, in order to describe the coalescence of two cells as a smooth process. We have adopted random patterns with about 6000 cells as the initial state of the computer simulation. The simulated patterns show that as time goes on cells coarsen and the shape of cells changes from a nearly round shape to various shapes. At long times, the pattern of the system develops into a self-similar pattern (scaling

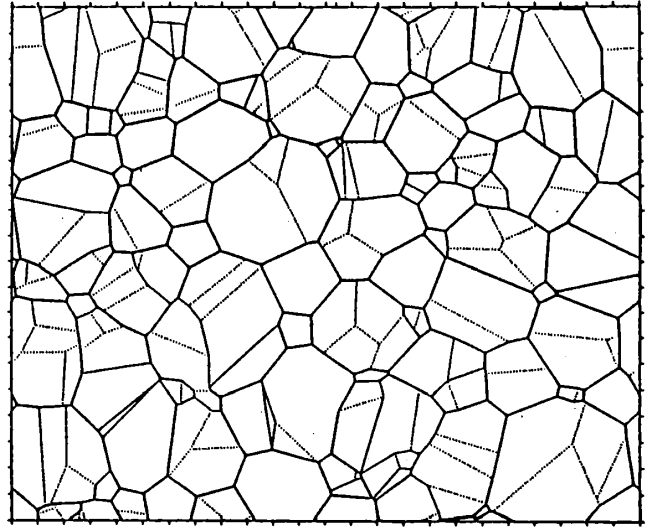


Fig.1 Snapshot of cell structure. Solid line:high and low energy boundary. Dotted line:pseudo boundary.

pattern). Figure 1 shows the scaling pattern where the shape of cells is more diverse than in the isotropic case. We show in Fig.2 the abundance ratios of the low energy boundary ($\sigma/3$), R_{LB} for the total length and R_{NB} for the total number. We can see that both gradually approach constants, $R_{LB}^* = 0.213$ and $R_{NB}^* = 0.117$, with increasing time. This supports the existence of the scaling state in the anisotropic system. The characteristic length of the system is the average cell radius $\bar{R}(t)$, which increases with $t^{1/2}$ at long times as in the isotropic system. The distribution functions for the cell edge-number and the cell size also show the scaling property and become broader than those of the isotropic system, demonstrating the diversity of the cell shape.

The solid circles in Fig. 3 show $\rho_{LB}(t) = (R_{LB}(t) - R_{LB}^*)/R_{LB}^*$ divided by $\rho_{LB}(0)$, while the solid line the stretched exponential $\exp[-(t/\tau)^\beta]$ fitted to them with $\tau = 30$ and $\beta = 0.56$. The fitting is satisfactory. The stretched exponential has been used as an empirical fit for the abnormal relaxation of disordered systems since F. Kohlrausch introduced it to describe strain relaxation in glassy fibers in 1863. Relaxation of some other quantities can be also well described by the stretched exponential. We have obtained that (τ, β) are (13, 0.84) for the average cell area \bar{R}^2 with an asymptote $\bar{R}^{*2} = 0.950t + 12.0$, (41, 0.59) for R_{NB} and (35, 0.48) for \bar{S} with $\bar{S}^* = 0.684$. Here \bar{S} is a quantity which gives the average roundness of a cell. It is calculated from the second-order moment and becomes the ratio of the short radius to the long radius in the ellipse approximation of cell shape. The relaxation time of the average cell area ($\tau_A = 13$) is much shorter than that of the other three quantities ($\tau_s = 35$, the mean of the three). Therefore this relaxation process can be divided into at least three stages. The characteristic length \bar{R} relaxes before τ_A , while the cell shape \bar{S} relaxes between τ_A and τ_s . The system is in the scaling state after τ_s .

We conclude : (1)The anisotropic cellular structure also shows the dynamical scaling, (2)The characteristic of the scaling state in the anisotropic system is diversity in the shape of cell, (3)Relaxation to the scaling state in the anisotropic system can be well described by the stretched exponential and has the stepwise character.

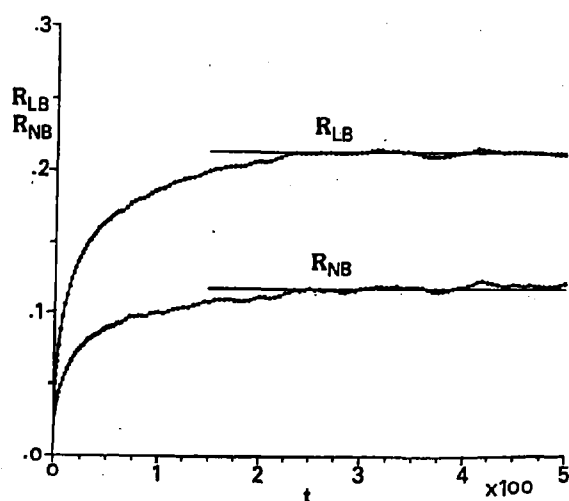


Fig.2 Abundance ratio of the low energy boundary.

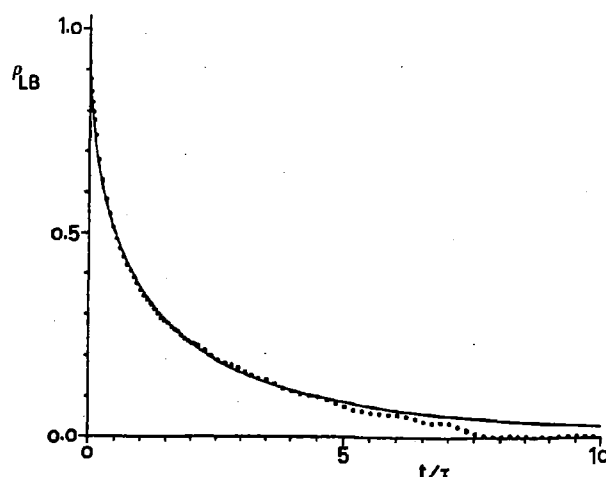


Fig.3 Relaxation of R_{LB} to the asymptote.

[1] Y.Saito and M.Enomoto, ISIJ International, 32, 267(1992).

[2] T.Nagai, K.Fuchizaki and K.Kawasaki, Physica A 204, 450(1994).